Journal of Drug Delivery Science and Technology 79 (2023) 104098

Contents lists available at ScienceDirect

Journal of Drug Delivery Science and Technology

journal homepage: www.elsevier.com/locate/jddst

Folic acid grafted aminated zeolitic imidazolate framework (ZIF-8) as pH responsive drug carrier for targeted delivery of curcumin

Reshmi R. [a,*], Jiju K.R. [b], Suma S. [c], Anoop S. Nair [d]

[a] Department of Chemistry, Sree Narayana College, Chengannur, Alaphuzha, 689508, Kerala, India
[b] Department of Chemistry, Sree Narayana College, Alathur, Palakkad, 678682, Kerala, India
[c] Department of Chemistry, Sree Narayana College, Chempazhanthy, Trivandrum, 695587, Kerala, India
[d] Department of Chemistry, NSS College, Nemmara, Palakkad, 678508, Kerala, India

ARTICLE INFO

Keywords:
Drug delivery systems
Zeolitic imidazolate framework-8(ZIF-8)
Folic acid
Curcumin

ABSTRACT

Smart drug delivery systems responding to pH gradient between physiological conditions and acidic conditions in tumor cells are very crucial for treating cancer. This article describes the process of developing, zeolitic imidazolate framework (ZIF-8) based novel pH responsive drug carrier for the targeted delivery of curcumin (CUR). To enable folic acid (FA) conjugation the surface of ZIF-8 was modified through amination. The so developed CUR loaded folic acid grafted aminated ZIF-8 (CUR@FA-g-AZIF-8) were characterized with UV–Visible, FT-IR, PXRD, SEM, TGA, TEM and BET analysis. It shows high drug loading efficiency and good chemical stability. *In vitro* drug release studies of CUR from folic acid grafted aminated ZIF-8 (FA-g- AZIF-8) shows three times higher efficiency in acidic pH (5) than in normal physiological conditions (pH 7.4). The potential cytotoxicity was evaluated by MTT assay on HeLa cells, CUR@FA-g-AZIF-8 shows 76.8% cytotoxicity. The results show that FA-g-AZIF-8 is a promising drug carrier for targeted drug delivery.

1. Introduction

Metal-organic frameworks (MOFs) has become a wide range of research topic nowadays. MOF is composed of metals coordinated to organic ligands to form finite secondary building units (SBUs) and have immense contribution to material science, pharmaceutical science, and nanotechnology [1]. The presence of SBU's gives a geometrical shape which have numerous functionalities to MOF's. They are also called porous coordination polymers and possesses ultrahigh porosity and exceptional large surface area which give rise to low density and considerable mechanical and thermal stability [2]. The important application of MOF's is hydrogen storage, gas absorption and separation, drug release, catalytic reaction and other fields [3]. MOF faces a disadvantage as it has low aqueous stability which would lead to hydrolysis and decomposition in presence of moisture. As zeolite have high rigid structure, high aqueous stability and appropriate surface area, they had been widely used in chemical industry. Due to their rigid structure, pore size and eaze of functionalization, they can be modified by self-assembly method, Yaghi et al. designed and synthesized MOF with zeolite like structure (ZIF's) [4]. ZIFs are crystalline metal clusters bridged tetrahedrally *via* the imidazolate type of or self-assembled as M-IM-M structures were 'M' stands for tetrahedrally coordinated transition metal ions (Fe, Co, Cu, Zn) and 'IM' is the imidazole ligands. The angle of this structure is 145° to enable a zeolite like topology [4]. ZIF's exhibit properties of both MOF's and zeolite such as exceptional thermal and chemical stability, ultra-high surface area, high crystallinity, unimodal microspores and abundant functionalities [5]. Thus, it can be used in numerous fields including gas separations [6,7], catalysis [8], gas storage [9–11], chemical sensors [12,13] and drug delivery [14]. ZIF response to various stimuli like pH, singlet oxygen and redox potential gradient which leads to the characterization suitable for drug delivery.

ZIF-8 ($Zn[MeIM_2 = ZnC_8H_{10}N_4$; 2-MeIM = 2-Methylimidazolate) is typical type of ZIF's which exhibits a sodalite type structure. It has a high BET specific surface area (SSA) (2000 m^2/g) and permanent porosity from its uniformly sized pore cavities (=1.16 nm and pore volume of 0.60 cm^3/g) particularly desirable for many potential applications such as molecular gas storage separation by membrane sieving or Kinetic diffusion caging templating catalysis and shape selective distillation and sensing [15].

Several synthesis approaches of ZIF-8 have been proposed including solvothermal synthesis, hydrothermal synthesis, ultrasound synthesis, mechano chemical synthesis and accelerated aging methods [16]. A

* Corresponding author.
E-mail addresses: reshmimythri@gmail.com (R. R.), krjijukrjiju@gmail.com (J. K.R.), sumasncw@gmail.com (S. S.), anoopkkred@yahoo.co.in (A.S. Nair).

https://doi.org/10.1016/j.jddst.2022.104098
Received 21 September 2022; Received in revised form 6 December 2022; Accepted 18 December 2022
Available online 21 December 2022

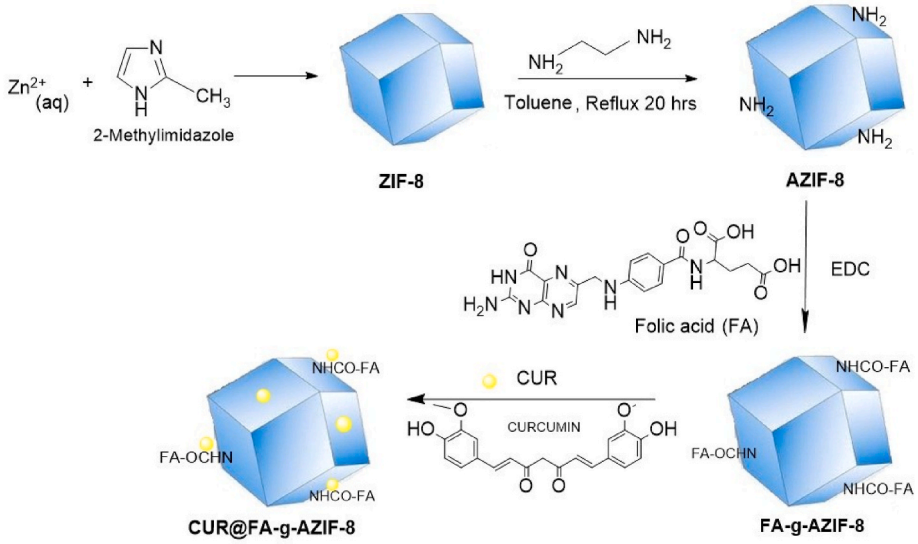

Fig. 1. Synthesis scheme of CUR@FA-g-AZIF-8

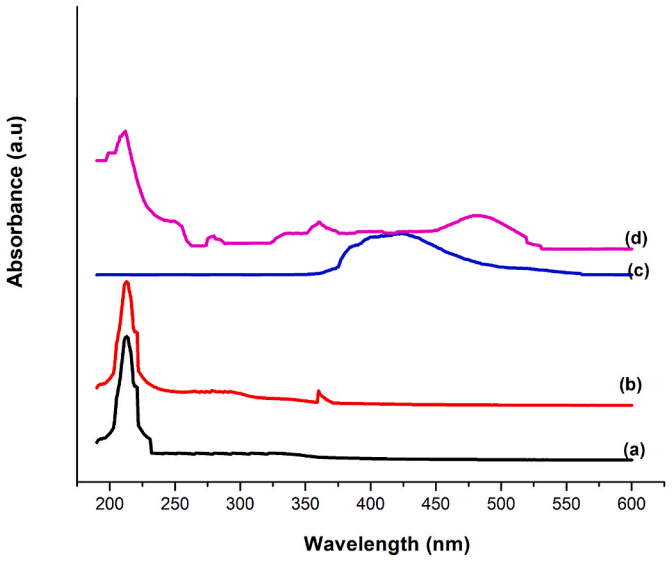

Fig. 2. UV plots of (a) ZIF-8, (b) FA-g-AZIF-8, (c) CUR and (d) CUR@FA-g-AZIF-8

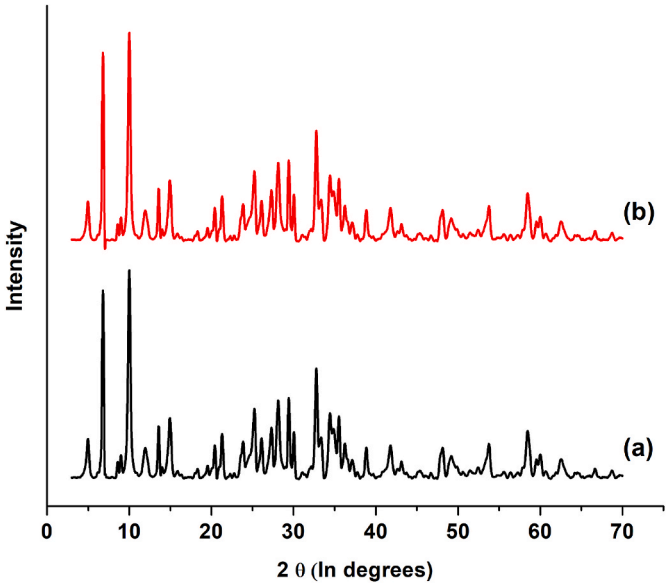

Fig. 3. XRD plots of (a) ZIF-8, (b) CUR@FA-g-AZIF-8

large quantity of ZIF-8 can be readily synthesized by simple mixing of precursors of zinc nitrate/acetate and 2-methylimidazole in a water or methanol solvent at room temperature [17]. Among all the MOFs ZIF-8 is very popular as pH responsive drug delivery system [18]. Sun et al. were first to use ZIF-8 as pH triggered DDS. About 70% of 5-fluorouracil was released in 72 h [19]. Later, Liedana et al. developed ZIF-8 framework, which could encapsulate 28% of caffeine [20]. Zhuang et al. synthesized doxorubin loaded ZIF-8 as pH responsive drug delivery system [21]. Zheng et al. reported pH responsive drug release using curcumin loaded ZIF-8 and studied the anticancer activity [22]. Ashish Tiwari et al. developed curcumin encapsulated ZIF-8 as stimuli responsive drug delivery system in which stimuli involves pH change and presence of biomimetic cell membrane like environment [23]. It is a widely used strategy that the drugs are targeting towards the cancer cells, in which the drug loaded NPs anchored with ligand can directly interact with receptors present or overly expressed on the surface of cancer cells. There are various reports in which modified MOFs have been developed for targeted delivery of the drug [24,25]. Some receptors like folate are over expressed in cancer cells but not in normal cells [26]. Folic acid shows high affinity to folate receptors and shows enhanced delivery to FR-positive tumor cells [27,28]. Folate receptors present at the surface of tumor cells combine with folic acid or its conjugate and are internalized to intracellular compartments [29]. In the acidic environment of tumor cells (pH = 5 5.5) the conjugation between folate conjugate and folate receptor breaks and folate receptors moves back to the surface of cell while folate conjugates get degraded [30,31]. Only very few works are reported so far in which FA conjugated ZIF-8 [32–34],since the surface modification of ZIF-8 with functional groups are quite difficult. In the present work, first ZIF-8 was surface modified through amination, then folic acid was conjugated and finally CUR was loaded. For the best of our knowledge no such work has been reported yet.

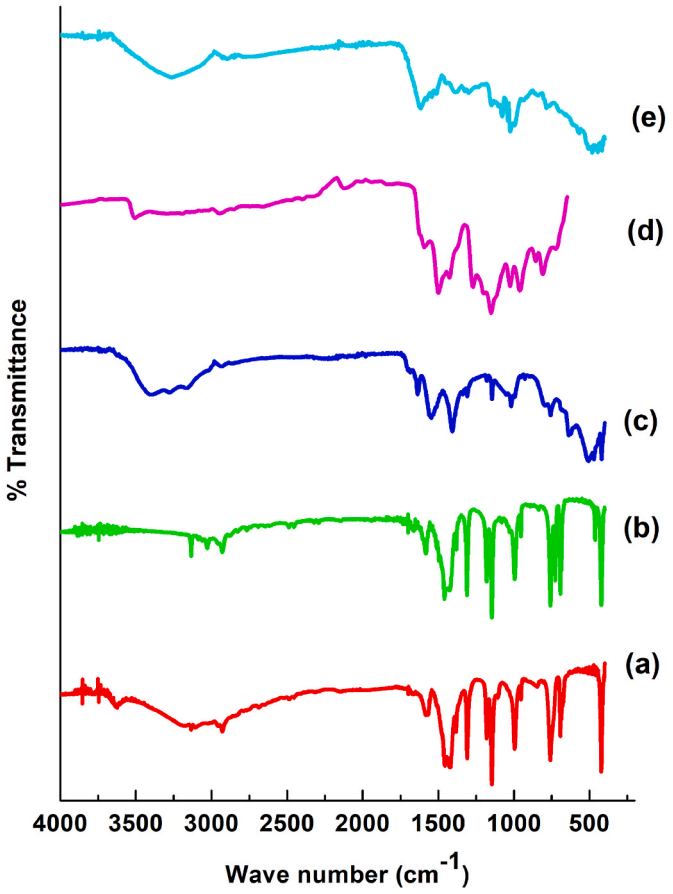

Fig. 4. FT-IR plots of synthesized samples (a) ZIF-8, (b) AZIF-8, (c) FA-g-AZIF-8, (d) CUR and (e) CUR@FA-g-AZIF-8

2. Material and methods

2.1. Materials

$Zn(NO_3)_2.6H_2O$, 2-Methylimidazole(2-MeIM), curcumin(CUR), Folic acid(FA), ethylene diamine, 1-Ethyl-3-(3-dimethylaminopropyl)carbodiimide (EDC).

2.2. Methods

2.2.1. Synthesis of ZIF-8

ZIF-8 were prepared based on previously reported method accordingly, 293 mg (9.8×10^{-4} mol) $Zn(NO_3)_2.6H_2O$ was dissolved in 10 mL DI water. Another solution containing 1.08 g 2-MeIM (1.3×10^{-2} mol) in 20 mL DI water were prepared. The first solution then added to the second without stirring at room temperature. $Zn(NO_3)_2.6H_2O$ and 2-MeIM were reacted in the 0.075: 1 ratio to get 0.075 mol of ZIF-8 as per the above calculations. After 24 h, the white precipitate was collected through centrifugation at a rate of 7000 rpm for 5 min and washed with DI water for 3 times [35].

2.2.2. Synthesis of aminated ZIF-8 (AZIF-8)

The surface modification of ZIF-8 was made based on a previously reported method. Briefly, before modification the synthesized ZIF-8 were dried at 100°C overnight. 2 g ZIF-8 (8.7×10^{-6} mmol)in 30 mL anhydrous toluene is mixed with 0.75 mmol of ethylene diamine and the mixture was refluxed for 20 h. The obtained AZIF-8 were centrifuged and washed with ethanol for three times [36]. 2.3 equivalence of $–NH_2$ per gram of AZIF-8 was obtained calorimetrically using ninhydrin test [37].

2.2.3. Folic acid conjugation to AZIF-8

Folic acid was conjugated to AZIF-8 through –CONH amide linkage be-tween –COOH group of FA with $–NH_2$ group of AZIF-8 [38]. FA acid grafted AZIF-8 (FA-g-AZIF-8) were prepared as follows, first 0.56 g FA (2 equivalence –COOH per gram) and 0.2 g EDC were suspended in 20 mL dimethyl sulphoxide (DMSO) and stirred for 2 h to get a homogeneous solution. A solution of 0.25 g (2.3 equivalence of $–NH_2$ per gram) AZIF-8 in 50 mL DI were prepared separately. The first solution was added dropwise to the second (1:1 molar ratio) with constant stirring and stirring continued for 16 more hrs. The resultant red colored solution was centrifuged and dried.

2.2.4. Preparation of CUR loaded FA-g-AZIF-8 (CUR@FA-g-AZIF-8)

CUR and FA-g-AZIF-8 were mixed in 2:1 ratio and the mixture was stirred for 8 h in a magnetic stirrer in dark [36]. The precipitate was collected, centrifuged and dried. Unreacted CUR was eliminated by washing with DI for three times as per the early reports [39]. Similarly, CUR were loaded to the as-synthesized ZIF-8 without any modifications for comparison. The various steps involved in the synthesis process is represented in the scheme (Fig. 1).

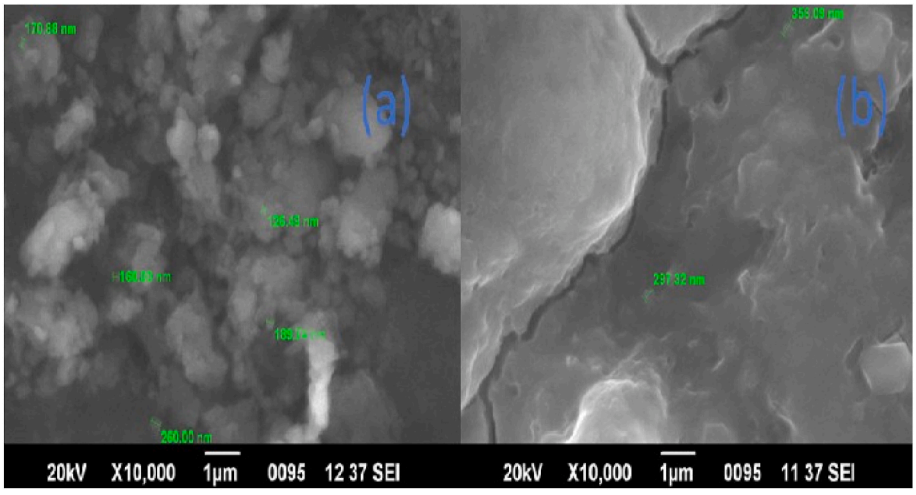

Fig. 5. SEM images of (a) ZIF-8, (b) CUR@FA-g-AZIF-8

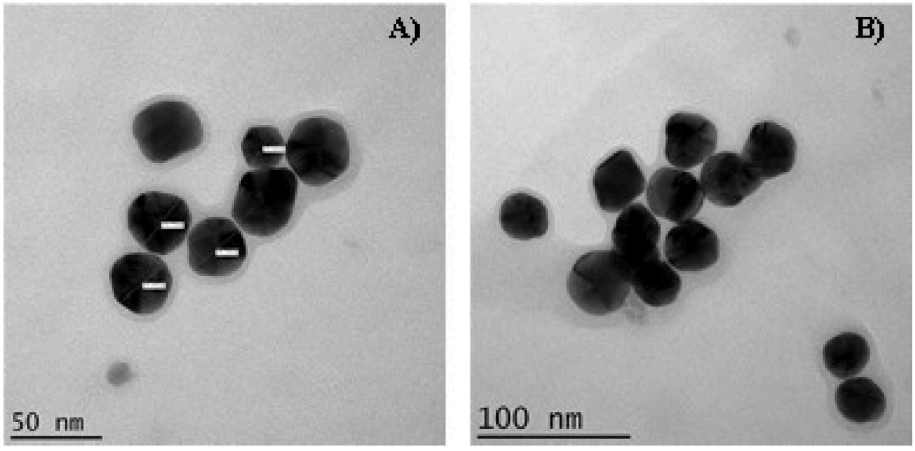

Fig. 6. TEM images of (a) ZIF-8, (b) CUR@FA-g-AZIF-8

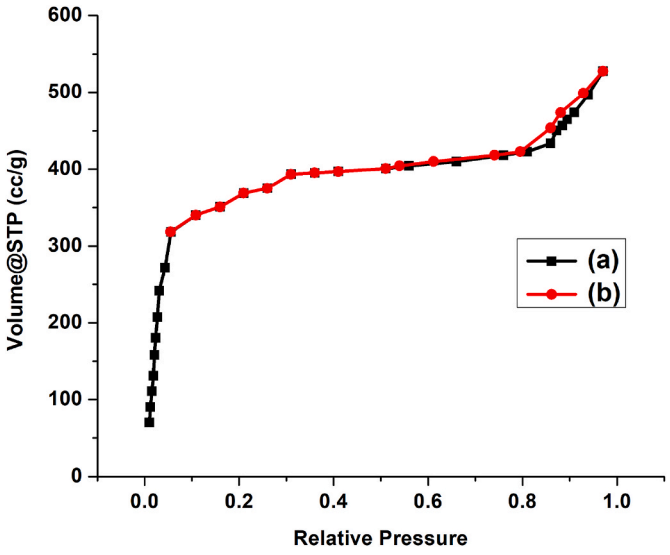

Fig. 7. N_2 adsorption-desorption isotherm of ZIF-8 (a)Adsorption isotherm (b) Desorption isotherm.

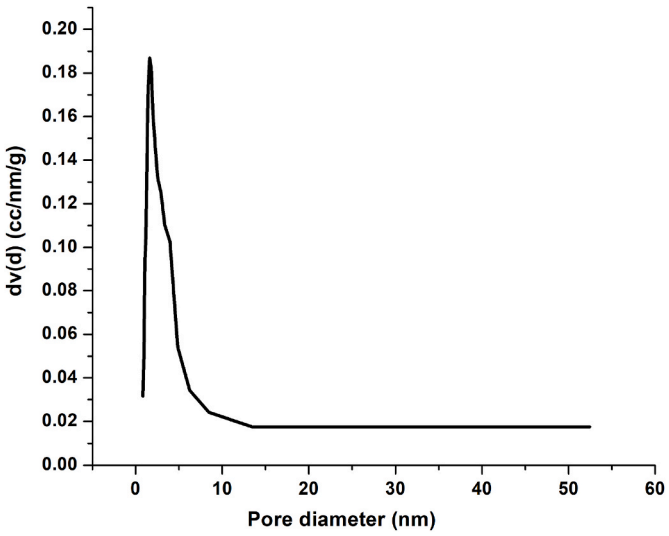

Fig. 9. Pore size distribution curve of CUR@FA-g-AZIF-8

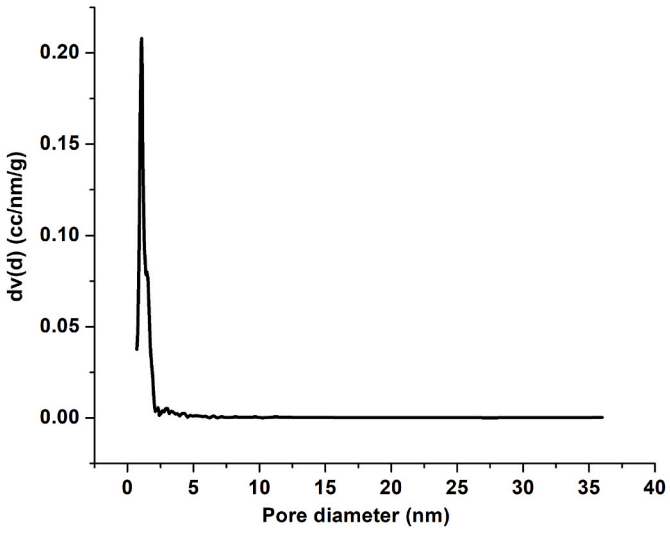

Fig. 8. Pore size distribution curve of ZIF-8.

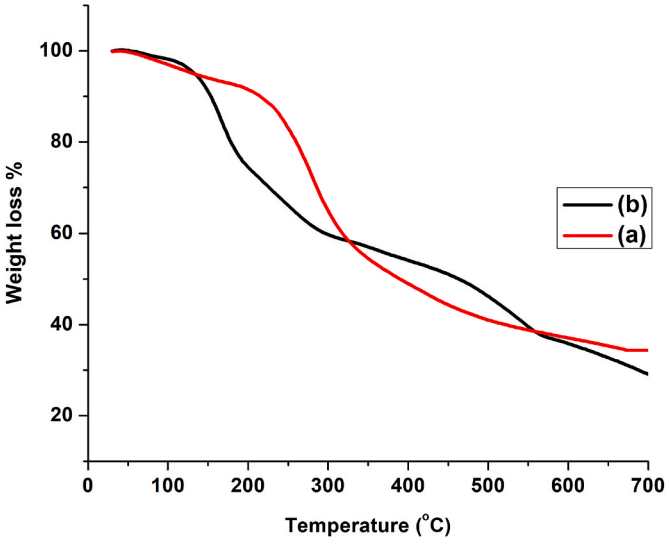

Fig. 10. TGA curves of (a) ZIF-8, (b) CUR@FA-g-AZIF-8

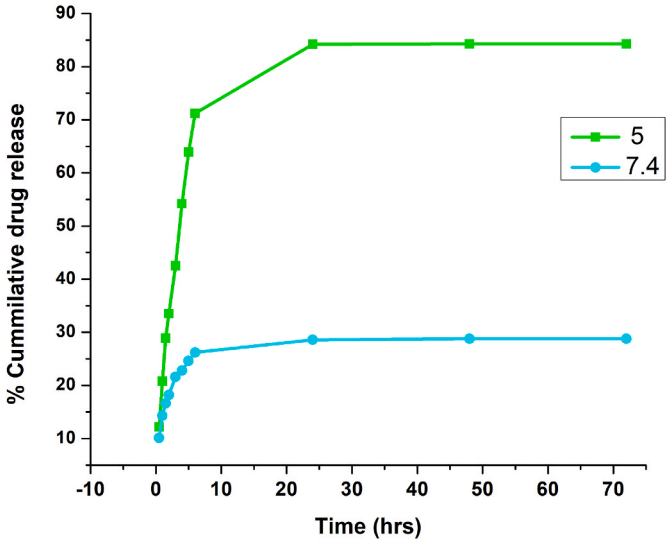

Fig. 11. Drug release profile of CUR@FA-g-AZIF-8 at pH 5 and pH 7.4.

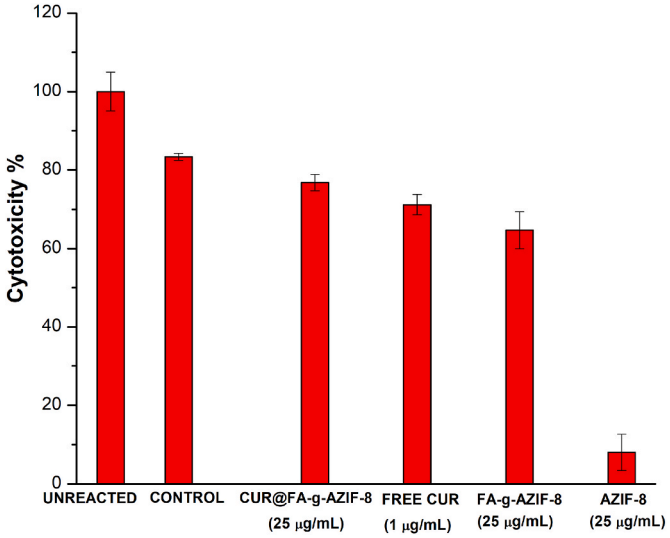

Fig. 12. Cytotoxicity of Free CUR, FA-g-AZIF-8, CUR@FA-g-AZIF-8 and AZIF-8 in cubated with HeLa cells for 48 h.

2.2.5. Drug release study

In vitro stimuli responsive drug release study from CUR@FA-g-AZIF-8 were performed under acidic (pH 5) and physiological conditions (pH 7.4) using PBS solutions at 37°C in a shaking incubator. 1 mL each of the release solutions were withdrawn at regular time interval and was replaced with same volume to maintain a constant volume. Amount of CUR released was determined using UV–Visible spectrophotometer with the absorbance at 425 nm. For pure CUR, the absorption peak at 425 nm was used to make a calibration curve by serial dilution of known concentration of CUR. The amount of drug loaded to FA-g-AZIF-8 and ZIF-8 were also calculated with this standard calibration curve. Data were expressed as means of three separate experiments, and were compared by analysis of variance (ANOVA). A p-value <0.05 was considered statistically significant in all cases.

2.2.6. Cytotoxicity studies

3-(4,5-dimethylthiazole-2-yl)-2,5-diphenyl tetrazolium (MTT) assay was performed on human cervical carcinoma cells (HeLa cells) with AZIF-8, free CUR, FA-g-AZIF-8 and CUR@FA-g-AZIF-8 to evaluate cytotoxicity. AZIF-8, FA-g-AZIF-8 and CUR@FA-g-ZIF-8 weretaken at a concentration of 25 μg/mL, while the free CUR concentration was fixed as 1 μg/mL. Cells were first seeded in 12-well plates (50,000 cells/well) and incubated in 5% CO_2 environment at 37°C for 24 h. Then, the cells were treated with FA-g-AZIF-8, CUR and CUR loaded FA-g-AZIF-8, the untreated cells as control, cultured for 48 h. Then MTT solution (0.5 mg/mL) was added to each well and incubated for 3 h. After removing MTT reagent, 100μL DMSO was added and optical density (OD) measured at 570 nm on a spectrophotometer and % cell viability was calculated [40].

2.2.7. Characterization

The prepared materials were characterized using UV–Vis spectrophotometer, FT-IR, X-ray diffraction, Scanning electron microscope, N_2 adsorption studies and Thermogravimetric analyzer. The PXRD analysis were performed with Bruker D8 ADVANCE with DAVINCI. The Fourier transform infrared spectroscopy was studied using Thermo scientific Nicolet iS50 instrument. SEM was performed with Carl Zeiss EVO 18 Research instrument. Thermogravimetric analysis were conducted using PerkinElmer STA 8000. The samples were heated in a flow of air with a ramp of 5°C per minute up to 800°C. N_2 adsorption studies using Quanta chrome instruments Nova Touch lx4 Model at 77 K. The samples were heated at 150°C for 3 h for de-gasification before the BET analysis.

3. Results and discussions

The UV–Vis absorption peaks of ZIF-8, FA-g-AZIF8, CUR and CUR@

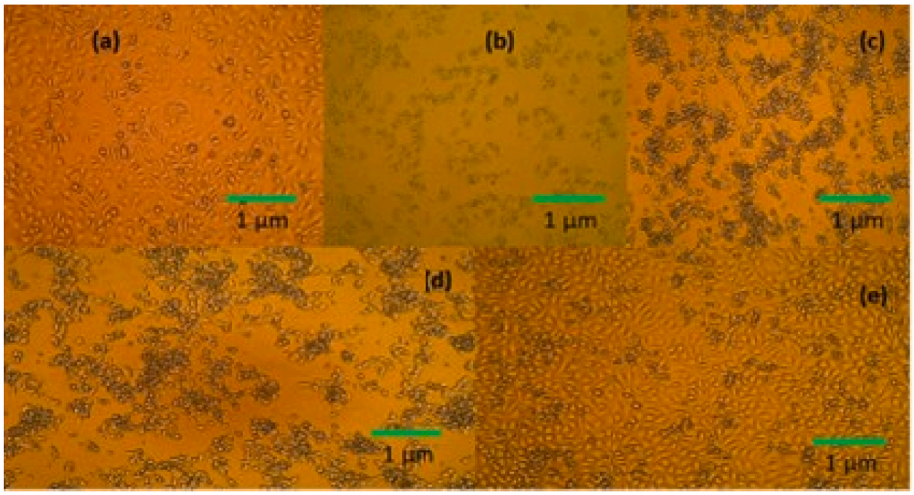

Fig. 13. Optical photographs of (a) Untreated, (b) Std. control (c) Free CUR, (d) CUR@FA-g-AZIF-8 and (e) AZIF-8 in HeLa cells.

FA-g-AZIF8 are given in Fig. 2. In the spectra of ZIF-8, the characteristic absorption peak at 213 nm was observed [23]. In the curve FA-g-AZIF8, absorption peaks at 280 and 360 nm which is the characteristic peaks of FA was observed [41]. In the curve of CUR@ FA-g-AZIF8 in addition to the peak of ZIF-8 and FA, the characteristic peak of CUR shifted from 425 nm to 480 nm which indicates successful loading of CUR [42].

The crystal structure of ZIF-8 and CUR@FA-g-AZIF-8 was determined by PXRD(Fig. 3). The XRD pattern of ZIF-8 matched well with reported literature [43,44]. The characteristic peaks of ZIF- 8 at 2 values of 7.1, 10.24, 12.86 and 18.2 correspond to (110), (200), (211) and (222) index planes respectively. There was no change in the XRD pattern of CUR@FA-g-AZIF-8 as compared to ZIF-8 indicating the framework stability and minimum impact on its crystallinity [36,45].

The various synthesis steps were proven by FT-IR analysis (Fig. 4). From the FT-IR spectra of ZIF-8 (Fig. 4a) the bands at 3136 cm^{-1} and 2925 cm^{-1} corresponds to the aromatic and aliphatic C–H stretching vibration of imidazole ring, respectively. The peak at 1587 cm^{-1} is due to C = N stretching vibration. The peak at 422 cm^{-1} is related to the Zn–N symmetric stretching. The C–N stretching vibration is appeared at 1100 and 1400cm^{-1} [46,47]. The absorption peak at 3270 cm^{-1} corresponds to N–H stretching vibrations and in the range of 1526–1540 due to N–H bending vibrations of AZIF-8 (Fig. 4b) [48,49]. From the FT-IR spectra of FA-g-AZIF-8 (Fig. 4c), in addition to the absorption bands of ZIF-8 and AZIF-8, the –CONH amide band at 1647 cm^{-1} and the –NH bending vibrations at 1535 cm^{-1} indicates the successful conjugation of –COOH group of FA with $–NH_2$ group of AZIF- 8 [34,50]. In CUR spectra (Fig. 4d) the peak at 3515 cm^{-1} is due to –OH group of phenol. Other peaks at 1152,1279 and 1513 cm^{-1} are due to C–O–C aromatic stretching, C–O aromatic stretching and C═C a stretching of benzene ring [51]. In the spectra of CUR@FA-g-AZIF-8 (Fig. 4e) a sharp decrease was observed in the range of 3400–3100 cm^{-1} relating to –OH band in CUR, which confirms a strong H-bonding between phenolic group in CUR and - CONH group on the surface of FA-g-AZIF-8 [52,53]. All these indicates the successful loading of CUR on to the modified systems.

SEM images of ZIF-8 and CUR@FA-g-AZIF-8 are given Fig. 5. As per the early reports ZIF-8 have rhombic dodecahedron geometry [47,54]. From the SEM images of ZIF-8 (Fig. 5a) it is very clear that they possess cubic geometry. There is no significant change in the morphology of the obtained CUR@FA-g-AZIF-8 as compared with ZIF-8 which proves the structural rigidity of ZIF-8 even after the modifications.

The TEM images of pure ZIF-8 and CUR@FA-g-AZIF-8 were obtained as shown in Fig. 6. As expected, ZIF-8 exhibited a cuboid geometry and serves as a proof for the successful synthetic procedure reported elsewhere [55]. It showed a maxi-mum size of 34 nm. However, on modification and loading with CUR, its size increased to 51 nm and morphology changed minimalist to a spheroid form. Further, increase in size and change in morphology might be due to the incorporation of aromatic groups of FA and due to amination. The small increase in size from 34 to 51 nm might be also evidence for the surface loading of CUR onto ZIF-8.

Surface area and porosity of ZIF-8 were studied using N_2 adsorption-desorption isotherms (Fig. 7). The BET adsorption isotherms are linear curves at low relative pressures as shown in Fig. 7 indicating a type I isotherm [47]. During the adsorption experiments there was a significant increase in the nitrogen uptakes confirms the micro porosity of ZIF-8. The measured BET specific surface area of 1198 m^2/g is closely related with those prepared ZIF-8 in aqueous solutions [44,56].

From the pore size distribution curves of ZIF-8 CUR@FA-g-AZIF-8 (Figs. 8 and 9) it is very clear that the prepared materials are micro porous in nature. The peak maxima were observed at less than 2 nm, which is the characteristic nature of micro porous materials. The total pore volume was calculated as 0.62 cc/g for ZIF-8 and 0.58 cc/g for CUR@FA-g-AZIF-8 which closely related to the early reported values [35]. Since there is no considerable decrease in pore volume for CUR@FA-g-AZIF-8 it may be assumed that most of the CUR get loaded on the surface of FA-g-AZIF-8.

TGA was performed and the results are shown in Fig. 10. Thermal studies of ZIF-8 were well matched with the reported value [44,57]. The first weight loss is due to the removal of water and other unreacted molecules. A sharp weight loss of 58% between 200 °C to 700^o C is due to the degradation of structure and complete decomposition of organic linkers (2-MIM). This is in good agreement with the calculated value of 62.8% [54]. The final weight loss of 58% proves the complete transformation of ZIF-8 (molar mass 227.6) to ZnO (molar mass 81) [58]. The residual mass of 34.4% is in good agreement with the residual mass of ZnO (36%) [44]. The CUR@FA-g-AZIF-8 framework showed a weight loss from 200 °C as a result of decomposition of CUR started and decomposed completely between 200 and 550 °C [23].

FA-g-AZIF-8 shows greater drug loading efficiency of 91.6% compared to ZIF-8 (85.4%). This is due to the surface modification and thereby the formation of amide linkages, which forms electrostatic interaction with –OH and –CO (carbonyl) group of CUR [36,59,60]. Drug release studies from CUR@FA-g-AZIF-8 were performed for 72 h. The resultant cumulative drug release is shown in Fig. 11. From the drug release profile curve, it is clear that about 84% drug was released in acidic conditions (pH 5) while in the physiological conditions (pH 7.4) the release was only 28.5%. This shows a three-fold increase in drug release under acidic medium as compared to physiological conditions. Since tumor cells are acidic, imidazolate ligands get protonated and the linkage between Zn and imidazolate breaks, there by ZIF-8 framework get collapsed. Similarly, protonation breaks the electro-static linkage between CUR and –CONH at the surface of ZIF-8, both these leads to an effective increase in CUR release. Thus, the prepared compound is an excellent drug carrier.

The potential cytotoxicity of free CUR, AZIF-8, FA-g-AZIF-8 and CUR@FA-g-AZIF-8 was evaluated by MTT assay using HeLa cells, the results were shown in Fig. 12. As shown in the Fig, AZIF-8, FA-g-AZIF-8, free CUR and CUR@FA-g-AZIF-8 shows about 8%, 64.7%, 71.2% and 76.8% of cytotoxicity against HeLa cells. AZIF-8, FA-g-AZIF-8 and CUR@FA-g-AZIF-8 were treated with HeLa cells at a concentration of 25 μg/mL, while free CUR were treated at a concentration of 1 μg/mL. The better cytotoxicity of CUR@FA-g-AZIF-8 compared with free CUR may be both due to slow release of CUR from FA-g-AZIF-8 as well as due to the targeting ability of folic acid [32]. Optical photographs of MTT assay results of free CUR, CUR@FA-gAZIF-8 and AZIF-8 are given in Fig. 13.

4. Conclusion

In the present work, first the surface of ZIF-8 was modified through amination and then folic acid was conjugated. Thus, we could prepare a novel folic acid conjugated aminated ZIF-8 drug delivery system for the targeted delivery of CUR. ZIF-8 possess pH stimuli responsive behavior which has been taken as advantage to trigger release of drug in response to external

pH changes in tumor cells compared with physiological conditions. Since tumor cells are acidic, imidazolate get protonated and the linkage between Zn and imidazolate breaks, there by ZIF-8 get collapsed. Similarly, protonation breaks the electrostatic linkage between CUR and –CONH at the surface of ZIF-8, both these lead to an effective increase in CUR release. The prepared DDS shows high drug loading capacity (91.6%). *In vitro* drug release studies showed three times greater (88%) drug release in acidic pH compared to physiological conditions (28%). CUR@FA-g-AZIF-8 showed 76.8% cytotoxicity at a concentration of 25 μg/mL against HeLa cells, on the other hand free CUR shows 71.2% cytotoxicity (1 μg/mL), which demonstrated the targeting ability of prepared compound FA-g-AZIF-8. All these suggests that the so prepared drug delivery system is an excellent candidate for the pH stimuli responsive and targeted delivery of CUR.

Declaration of competing interest

There is no conflict of interest for the authors.

Data availability

Data will be made available on request.

Acknowledgements

Here we acknowledge Sree Narayana College for Women, Kollam for providing research facility.

References

[1] A.K. Cheetham, C. Rao, R.K. Feller, Structural diversity and chemical trends in hybrid inorganic–organic framework materials, Chem. Commun. 46 (2006) 4780–4795.
[2] D. Fairen-Jimenez, S. Moggach, M. Wharmby, P. Wright, S. Parsons, T. Düren, Opening the Gate: Framework Flexibility in Zif-8 Explored by Experiments and Simulations.
[3] P. Jiang, Y. Hu, G. Li, Biocompatible au@ ag nanorod@ zif-8 core-shell nanoparticles for surface-enhanced Raman scattering imaging and drug delivery, Talanta 200 (2019) 212–217.
[4] R. Banerjee, A. Phan, B. Wang, C. Knobler, H. Furukawa, M. O'Keeffe, O.M. Yaghi, High-throughput synthesis of zeolitic imidazolate frame- works and application to co2 capture, Science 319 (5865) (2008) 939–943.
[5] F. Wang, Y.-X. Tan, H. Yang, H.-X. Zhang, Y. Kang, J. Zhang, A new approach towards tetrahedral imidazolate frameworks for high and selective co 2 uptake, Chem. Commun. 47 (20) (2011) 5828–5830.
[6] Y. Li, F. Liang, H. Bux, W. Yang, J. Caro, Zeolitic imidazolate frame- work zif-7 based molecular sieve membrane for hydrogen separation, J. Membr. Sci. 354 (1–2) (2010) 48–54.
[7] Y. Liu, E. Hu, E.A. Khan, Z. Lai, Synthesis and characterization of zif- 69 membranes and separation for co2/co mixture, J. Membr. Sci. 353 (1–2) (2010) 36–40.
[8] C. Chizallet, S. Lazare, D. Bazer-Bachi, F. Bonnier, V. Lecocq, E. Soyer, A.-A. Quoineaud, N. Bats, Catalysis of transesterification by a non-functionalized metal-organic framework: acido-basicity at the external sur- face of zif-8 probed by FT-IR and ab initio calculations, J. Am. Chem. Soc. 73 (2004) 81–88.
[9] H. Wu, W. Zhou, T. Yildirim, Hydrogen storage in a prototypical zeolitic imidazolate framework-8, J. Am. Chem. Soc. 129 (17) (2007) 5314–5315.
[10] L.J. Murray, M. Dincă, J.R. Long, Hydrogen storage in metal–organic frameworks, Chem. Soc. Rev. 38 (5) (2009) 1294–1314.
[11] S. Ma, H.-C. Zhou, Gas storage in porous metal–organic frameworks for clean energy applications, Chem. Commun. 46 (1) (2010) 44–53.
[12] G. Lu, J.T. Hupp, Metal- organic frameworks as sensors: a zif-8 based fabry- Pérot device as a selective sensor for chemical vapors and gases, J. Am. Chem. Soc. 132 (23) (2010) 7832–7833.
[13] B.V. Harbuzaru, A. Corma, F. Rey, J.L. Jordá, D. Ananias, L.D. Car- los, J. Rocha, A miniaturized linear pH sensor based on a highly pho toluminescent self-assembled europium (iii) metal–organic framework, Angew. Chem. Int. Ed. 48 (35) (2009) 6476–6479.
[14] Q. Wang, Y. Sun, S. Li, P. Zhang, Q. Yao, Synthesis and modification of zif-8 and its application in drug delivery and tumor therapy, RSC Adv. 10 (62) (2020) 37600–37620.
[15] S. Gadipelli, W. Travis, W. Zhou, Z. Guo, A thermally derived and optimized structure from zif-8 with giant enhancement in co 2 uptake, Energy Environ. Sci. 7 (7) (2014) 2232–2238.
[16] Y.-R. Lee, M.-S. Jang, H.-Y. Cho, H.-J. Kwon, S. Kim, W.-S. Ahn, Zif- 8: a comparison of synthesis methods, Chem. Eng. J. 271 (2015) 276–280.
[17] H. Kaur, G.C. Mohanta, V. Gupta, D. Kukkar, S. Tyagi, Synthesis and characterization of zif-8 nanoparticles for controlled release of 6- mercaptopurine drug, J. Drug Deliv. Sci. Technol. 41 (2017) 106–112.
[18] S. Keskin, S. Kızılel, Biomedical applications of metal organic frame- works, Ind. Eng. Chem. Res. 50 (4) (2011) 1799–1812.
[19] C.-Y. Sun, C. Qin, X.-L. Wang, G.-S. Yang, K.-Z. Shao, Y.-Q. Lan, Z.-M. Su, P. Huang, C.-G. Wang, E.-B. Wang, Zeolitic imidazolate framework-8 as efficient ph-sensitive drug delivery vehicle, Dalton Trans- actions 41 (23) (2012) 6906–6909.
[20] N. Liédana, A. Galve, C. Rubio, C. Tellez, J. Coronas, Caf@ zif-8: one- step encapsulation of caffeine in MOF, ACS Appl. Mater. Interfaces 4 (9) (2012) 5016–5021.
[21] J. Zhuang, C.-H. Kuo, L.-Y. Chou, D.-Y. Liu, E. Weerapana, C.-K. Tsung, Optimized metal–organic-framework nanospheres for drug delivery: evaluation of small-molecule encapsulation, ACS Nano 8 (3) (2014) 2812–2819.
[22] M. Zheng, S. Liu, X. Guan, Z. Xie, One-step synthesis of nanoscale zeolitic imidazolate frameworks with high curcumin loading for treatment of cervical cancer, ACS Appl. Mater. Interfaces 7 (40) (2015) 22181–22187.
[23] A. Tiwari, A. Singh, N. Garg, J.K. Randhawa, Curcumin encapsulated zeolitic imidazolate frameworks as stimuli responsive drug delivery system and their interaction with biomimetic environment, Sci. Rep. 7 (1) (2017) 1–12.
[24] H. Chen, L.Q. Xie, J. Qin, Y. Jia, X. Cai, W. Nan, W. Yang, F. Lv, Q.Q. Zhang, Surface modification of PLGA nanoparticles with biotinylated chitosan for the sustained in vitro release and the enhanced cyto- toxicity of epirubicin, Colloids Surf., B: Bio. interfac. 138 (2016) 1–9.
[25] S. Haddad, I. Abanades Lazaro, M. Fantham, A. Mishra, J. Silvestre- Albero, J. W. Osterrieth, G.S. Kaminski Schierle, C.F. Kaminski, R. Forgan, D. Fairen-Jimenez, Design of a functionalized metal–organic framework system for enhanced targeted delivery to mitochondria, J. Am. Chem. Soc. 142 (14) (2020) 6661–6674.
[26] S.D. Weitman, R.H. Lark, L.R. Coney, D.W. Fort, V. Frasca, V.R. Zurawski Jr., B. A. Kamen, Distribution of the folate receptor gp38 in normal and malignant cell lines and tissues, Cancer Res. 52 (12) (1992) 3396–3401.
[27] A.R. Hilgenbrink, P.S. Low, Folate receptor-mediated drug targeting: from therapeutics to diagnostics, J. Pharmaceut. Sci. 94 (10) (2005) 2135–2146.
[28] Y. Tsume, J.M. Hilfinger, G.L. Amidon, Enhanced cancer cell growth inhibition by dipeptide prodrugs of floxuridine: increased transporter affinity and metabolic stability, Mol. Pharm. 5 (5) (2008) 717–727.
[29] A.C. Antony, The Biological Chemistry of Folate Receptors, 1992.
[30] J. Sudimack, R.J. Lee, Targeted drug delivery via the folate receptor, Adv. Drug Deliv. Rev. 41 (2) (2000) 147–162.
[31] Y. Lu, P.S. Low, Folate-mediated delivery of macromolecular anticancer therapeutic agents, Adv. Drug Deliv. Rev. 54 (5) (2002) 675–693.
[32] J. Bi, Y. Lu, Y. Dong, P. Gao, Synthesis of folic acid-modified dox@ zif-8 nanoparticles for targeted therapy of liver cancer, J. Nanomater (2018), 1357812, 1-5.
[33] L. Gao, Z. Wu, A.-R. Ibrahim, S.-F. Zhou, G. Zhan, Fabrication of folic acid-decorated hollow zif-8/au/cus nanocomposites for enhanced and selective anticancer therapy, ACS Biomater. Sci. Eng. 6 (11) (2020) 6095–6107.
[34] J. Yan, C. Liu, Q. Wu, J. Zhou, X. Xu, L. Zhang, D. Wang, F. Yang, H. Zhang, Mineralization of ph-sensitive doxorubicin prodrug in zif-8 to enable targeted delivery to solid tumors, Anal. Chem. 92 (16) (2020) 11453–11461.
[35] M. Jian, B. Liu, R. Liu, J. Qu, H. Wang, X. Zhang, Water-based syn- thesis of zeolitic imidazolate framework-8 with high morphology level at room temperature, RSC Adv. 5 (60) (2015) 48433–48441.
[36] A. Ghaee, M. Karimi, M. Lotfi-Sarvestani, B. Sadatnia, V. Hoseinpour, Preparation of hydrophilic polycaprolactone/modified zif-8 nanofibers as a wound dressing using hydrophilic surface modifying macromolecules, Mater. Sci. Eng. C 103 (2019), 109767.
[37] Y. Sun, F. Kunc, V. Balhara, B. Coleman, O. Kodra, M. Raza, M. Chen, A. Brinkmann, G.P. Lopinski, L.J. Johnston, Quantification of amine functional groups on silica nanoparticles: a multi-method approach, Nanoscale Adv. 1 (4) (2019) 1598–1607.
[38] M.P. Daryasari, M.R. Akhgar, F. Mamashli, B. Bigdeli, M. Khoobi, Chitosan-folate coated mesoporous silica nanoparticles as a smart and ph-sensitive system for curcumin delivery, RSC Adv. 6 (107) (2016) 105578–105588.
[39] E. Gholibegloo, T. Mortezazadeh, F. Salehian, H. Forootanfar, L. Firoozpour, A. Foroumadi, A. Ramazani, M. Khoobi, Folic acid decorated magnetic nano sponge: an efficient nano system for targeted cur- cumin delivery and magnetic resonance imaging, J. Colloid Interface Sci. 556 (2019) 128–139.
[40] T. Mosmann, Rapid colorimetric assay for cellular growth and survival: application to proliferation and cytotoxicity assays, J. Immunol. Methods 65 (1–2) (1983) 55–63.
[41] Q. Jiang, S. Zheng, R. Hong, S. Deng, L. Guo, R. Hu, B. Gao, M. Huang, L. Cheng, G. Liu, et al., Folic acid-conjugated Fe_3O_4 magnetic nanoparticles for hyperthermia and mri in vitro and in vivo, Appl. Surf. Sci. 307 (2014) 224–233.
[42] R.N. Moussawi, D. Patra, Modification of nanostructured ZnO surfaces with curcumin: fluorescence-based sensing for arsenic and improving arsenic removal by ZnO, RSC Adv. 6 (21) (2016) 17256–17268.
[43] X. Fan, W. Wang, W. Li, J. Zhou, B. Wang, J. Zheng, X. Li, Highly porous zif-8 nanocrystals prepared by a surfactant mediated method in aqueous solution with enhanced adsorption kinetics, ACS Appl. Mater. Interfaces 6 (17) (2014) 14994–14999.
[44] A.F. Gross, E. Sherman, J.J. Vajo, Aqueous room temperature syn- thesis of cobalt and zinc sodalite zeolitic imidazolate frameworks, Dalton Trans. 41 (18) (2012) 5458–5460.
[45] T.A. Vahed, M.R. Naimi-Jamal, L. Panahi, Alginate-coated zif-8 metal- organic framework as a green and bioactive platform for controlled drug release, J. Drug Deliv. Sci. Technol. 49 (2019) 570–576.
[46] Y. Hu, H. Kazemian, S. Rohani, Y. Huang, Y. Song, In situ high pressure study of zif-8 by FT-IR spectroscopy, Chem. Commun. 47 (47) (2011) 12694–12696.
[47] M. He, J. Yao, Q. Liu, K. Wang, F. Chen, H. Wang, Facile synthesis of zeolitic imidazolate framework-8 from a concentrated aqueous solution, Microporous Mesoporous Mater. 184 (2014) 55–60.
[48] L. Xu, C. Li, K.S. Ng, In-situ monitoring of urethane formation by FT-IR and Raman spectroscopy, J. Phys. Chem. 104 (17) (2000) 3952–3957.
[49] Z. Zhang, S. Xian, Q. Xia, H. Wang, Z. Li, J. Li, Enhancement of co2 adsorption and co2/n2 selectivity on zif-8 via post synthetic modification, AIChE J. 59 (6) (2013) 2195–2206.
[50] J. Ji, D. Wu, L. Liu, J. Chen, Y. Xu, Preparation, characterization, and in vitro release of folic acid-conjugated chitosan nanoparticles loaded with methotrexate for targeted delivery, Polym. Bull. 68 (6) (2012) 1707–1720.
[51] R. Feng, Z. Song, G. Zhai, Preparation and in vivo pharmacokinetics of curcumin-loaded pcl-peg-pcl triblock copolymeric nanoparticles, Int. J. Nanomed. 7 (2012) 4089.
[52] A. Bolouki, L. Rashidi, E. Vasheghani-Farahani, Z. Piravi-Vanak, Study of mesoporous silica nanoparticles as nanocarriers for sustained release of curcumin, Int. J. Nanosci. Nanotechnol. 11 (3) (2015) 139–146.

[53] K. Webb, V. Hlady, P.A. Tresco, Relative importance of surface wettbility and charged functional groups on nih 3t3 fibroblast attachment, spreading, and cytoskeletal organization, J. Biomed. Mater. Res.: An Off. J. Soc. Biomater., The Japan. Soc. Biomater. Aust. Soc. Bio- mater. 41 (3) (1998) 422–430.
[54] J. Cravillon, S. Munzer, S.-J. Lohmeier, A. Feldhoff, K. Huber, M. Wiebcke, Rapid room-temperature synthesis and characterization of nanocrystals of a prototypical zeolitic imidazolate framework, Chem. Mater. 21 (8) (2009) 1410–1412.
[55] H. Zheng, Y. Zhang, L. Liu, W. Wan, P. Guo, A.M. Nystrom, X. Zou, One-pot synthesis of metal–organic frameworks with encapsulated target molecules and their applications for controlled drug delivery, J. Am. Chem. Soc. 138 (3) (2016) 962–968.
[56] Y. Pan, Y. Liu, G. Zeng, L. Zhao, Z. Lai, Rapid synthesis of zeolitic imidazolate framework-8 (zif-8) nanocrystals in an aqueous system, Chem. Commun. 47 (7) (2011) 2071–2073.
[57] K.S. Park, Z. Ni, A.P. Côté, J.Y. Choi, R. Huang, F.J. Uribe- Romo, H.K. Chae, M. O'Keeffe, O.M. Yaghi, Exceptional chemical and thermal stability of zeolitic imidazolate frameworks, Proc. Natl. Acad. Sci. USA 103 (27) (2006) 10186–10191.
[58] B. Xu, Y. Mei, Z. Xiao, Z. Kang, R. Wang, D. Sun, Monitoring the mally induced structural deformation and framework decomposition of zif-8 through in situ temperature dependent measurements, Phys. Chem. Chem. Phys. 19 (40) (2017) 27178–27183.
[59] S. Kaur, D. Rana, T. Matsuura, S. Sundarrajan, S. Ramakrishna, Preparation and characterization of surface modified electro spun membranes for higher filtration flux, J. Membr. Sci. 390 (2012) 235–242.
[60] A. Mukerjee, J.K. Vishwanatha, Formulation, characterization and evaluation of curcumin-loaded PLGA nanospheres for cancer therapy, Anti- Cancer Res. 29 (10) (2009) 3867–3875.